

RESISTANCE FORCE AND GROUND BEHAVIOR IN THRUST PROTECTION FOR BURIED PIPES USING GEOGRID GABION

*Hiroyuki Araki¹ and Daiki Hirakawa²

¹ Faculty of Engineering and Design, Kagawa University, Japan;

² Faculty of Science and Engineering, Chuo University, Japan

*Corresponding Author, Received: 30 Jun. 2020, Revised: 22 Jan. 2021, Accepted: 13 Feb. 2021

ABSTRACT: The bend section of a buried water supply pipeline transfers a thrust force to the ground. Thus, a concrete block is typically installed at the bend for protection. However, the concrete block may become unstable when the ground around the concrete block liquefies during an earthquake. In a previous study, we proposed the use of a geogrid gabion composed of a geogrid basket and gravel as a thrust-protection method. In this method, the geogrid gabion is placed on the ground in the direction of the thrust force. It is desirable for a geogrid gabion to be installed close to the pipe. However, the pipe and gabion must be separated for the effective compaction of soil around the pipe during construction. In this study, the effects of the horizontal distance on the thrust force protection performance of the geogrid gabion were evaluated by applying a horizontal force on a buried pipe model in a saturated ground model. The results revealed that the resistance force acting on the pipe increased regardless of the horizontal distance; the resistance force acting on the pipe was highest when the pipe moved close to the geogrid gabion. Based on the relationship between the resistance and the ground behavior, the resistance force was modeled as the sum of the passive earth pressure acting on the pipe and the resistance increment due to the passive earth pressure acting on the geogrid gabion.

Keywords: Buried pipe, Thrust force, Gabion, Resistance force, Strain distribution

1. INTRODUCTION

A thrust force is generated in the outward direction of the bend section of buried pipes, e.g., water supply pipelines. The pipe is normally designed to resist the passive earth pressure and circumferential surface friction acting on the bend section. If the thrust force is estimated to exceed the resistance due to the passive earth pressure and surface friction, a concrete block is typically installed in the bend section, as shown in Fig. 1a. The concrete block is installed to increase the resistance by expanding the passive earth pressure-receiving area and increasing the friction at the bottom due to its heavy weight. However, a concrete block is expected to have the following disadvantages: generating a high inertial force at the bend due to the heavy weight of the concrete block during an earthquake, and significantly decreasing the resistance to thrust force or the stabilization when the ground around the pipe is liquefied. For example, it has been reported that the bend section detached when the surrounding ground liquefied [1].

If the proximity section of the bend is straight with sufficient length, a certain section of a pipe, including the bend, maybe welded instead of installing a concrete block. In this method, the passive earth pressure acting on the entire welded section is larger than that acting only on the bend, and a larger resistance to the thrust force is estimated. However, some cases of pipe detachment

at the boundary between welded and non-welded sections during earthquakes have been reported, and the inaccuracy of the calculation of the passive earth pressure acting on the welded section has been pointed out [2].

Therefore, a new thrust-protection method is required. Kawabata et al. [3] proposed the use of a geogrid as a thrust-protection method. In this method, the geogrid is connected to the pipe on the inside of the bend to act as a lateral anchor. From the results of lateral load tests using a small-scale model [3] and a full-scale model [4], it was confirmed that the resistance force against the thrust force was increased by installing this method. Furthermore, the results of shaking table tests [5] revealed that the lateral displacement of a pipe protected with the geogrid is lower than that of a pipe protected with a concrete block.

In [6], we proposed a new thrust-protection method involving the use of a geogrid gabion installed in the passive area of the buried pipe as a pressure-receiving structure (Fig. 1b). It is assumed that the passive earth pressure acting on the geogrid gabion and the surface friction of the geogrid acted as the resistance force against the thrust force. The basket is made of a polymer geogrid to obtain long-term stability against environmental events. Gravel with high permeability is used as the filling material of the basket, which is expected to retain effective stress by dispersing excess pore water pressure during an earthquake. The geogrid gabion is also

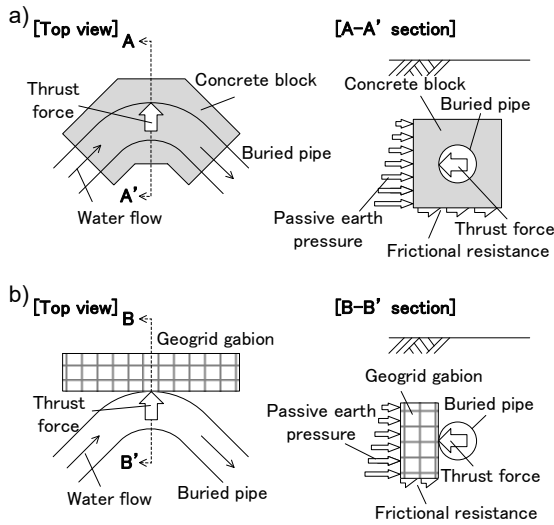


Fig. 1 Schematics of the a) concrete-block and b) proposed thrust-protection method [6,7].

expected to resist deformations due to the thrust force because the gravel is confined by the geogrid basket. In [6,7], we found that the displacement of the pipe protected with a geogrid gabbion was reduced and that the bottom part of the geogrid gabbion should be buried deeper than the pipe owing to its high stability; the large width of the geogrid gabbion prevented its rotation in the ground.

The geogrid gabbion should be installed close to a pipe but at a sufficient distance to allow the effective compaction of the soil around the pipe during construction. Therefore, the effects of the initial distance between a pipe and a geogrid gabbion should be clarified. Moreover, the resistance force acting on a pipe protected with a geogrid gabbion has hardly been discussed in the previous study. In this study, the resistance force acting on a pipe and ground behavior are discussed to further clarify the effects of thrust protection by conducting model experiments reproducing the horizontal distance between a pipe and a geogrid gabbion.

2. OUTLINE OF THE LATERAL LOAD TEST

2.1 Test Conditions

Lateral load tests were conducted to evaluate the resistance of a pipe and the behavior of the ground when a thrust force is applied laterally to the pipe. Although the ground is assumed to be three-dimensionally deformed when the thrust force is applied from the bend, it is difficult to evaluate the deformation of the ground owing to the complexity of the boundary conditions. For simplification, we modeled the model as a plane strain problem, with the cross-section B-B', as shown in Fig. 1b [6,7].

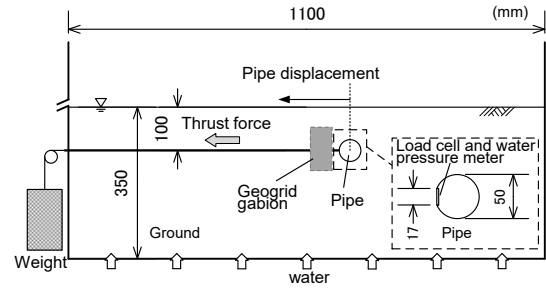


Fig. 2 Schematic of the lateral load test set-up.

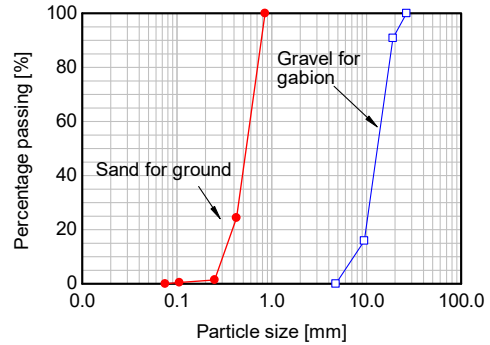


Fig. 3 Particle size distribution.

Figure 2 shows a schematic of the lateral load test set-up. The pipe model was loaded laterally inside the ground model constructed in a testing box, regarding Itani et al. [8]. To evaluate the effects of the initial horizontal distance between a geogrid gabbion and a pipe, several tests with different distances were conducted as described below.

The ground model was constructed with Mikawa silica sand No. 5 (soil particle density, $\rho_s = 2.675 \text{ g/cm}^3$) with the particle size distribution shown in Fig. 3. The maximum dry density and the optimum water content of the silica sand evaluated by the Proctor compaction test using A-a method according to JIS A 1210 [9] were 1.525 g/cm^3 and 14.7%, respectively. The ground model was constructed by wet tamping using silica sand with a water content of 13% to achieve a compaction layer thickness of 50 mm and a dry density of 1.296 g/cm^3 . The internal friction angle of the silica sand evaluated by consolidated-drained triaxial compression test according to JGS 0524-2009 [10] was 34.8 degrees under the condition of a dry density of 1.296 g/cm^3 .

The pipe model was designed as a straight cylinder with a diameter of 50 mm and a length of 390 mm. The pipe model had a smooth surface and was buried in the ground model at a depth of 100 mm from the ground surface. A simulated thrust force was applied laterally to the pipe model through a stainless-steel loading shaft, and the displacement of the loading shaft was measured as the pipe displacement d_p . A pore water pressure

meter and a load cell with a 17 mm width pressure plate were installed on the side of the pipe model, as shown in Fig. 2. Under the loading of the simulated thrust force, the lateral earth stress σ_p and pore water pressure u_p acting on the pipe model were measured using a load cell and water pressure meter, respectively. The effective value of the lateral earth stress acting on the pipe model σ'_p is defined as $(\sigma_p - u_p)$.

The geogrid gabion model consisted of gravel ($\rho_s = 2.807 \text{ g/cm}^3$) and a polypropylene net, as shown in Fig. 4. The geogrid gabion had a height of 100 mm and a width of 50 mm. The particle size distribution of the gravel is shown in Fig. 3. The dry density of the whole gabion was set to approximately 1.4 g/cm^3 . The depth of the geogrid gabion model center from the ground surface was set to be the same as that of the pipe model. To prevent the migration of silica sand into the geogrid gabions, a non-woven fabric was laid on the upper surface. The non-woven fabric was not laid on the side and bottom sections to simplify the condition between the geogrid gabion and silica sand in the model test.

2.2 Test Cases and Procedure

Table 1 shows the parameters of the test cases considered. To reproduce the initial horizontal distance between the geogrid gabion model and the pipe model D_h , three cases with D_h values of 15, 50, and 100 mm were considered, as shown in Fig. 5. The smallest value of D_h was set to 15 mm to ensure good compaction around the pipe (case G3). Considering a pipe diameter D of 50 mm, the D_h values of 15, 50, and 100 mm represented as 0.3D, 1.0D, and 2.0D, respectively.

Assuming that the surface friction of the pipe model is small due to its smooth surface, it is estimated that the passive area of the ground in contact with the pipe mainly resists the thrust force when the geogrid gabion is not installed. The boundary of the passive area is assumed to be located around Line A, which is considered with the internal friction angle of the ground, as shown in Fig. 5. In cases G4 and G6, roughly half and most of the geogrid gabion, were placed outside the ground passive area in contact with the pipe. In this study, a total of four cases were analyzed, including the above three cases, and case N2 without a geogrid gabion. These test cases were set up for the relative comparison of the resistance force and ground behavior, hence the scale effects between the prototype and the model were not considered.

In the lateral load test, a simulated thrust force F was applied to the pipe model after the ground model was saturated with water. The simulated thrust force was loaded until the changes in the pipe

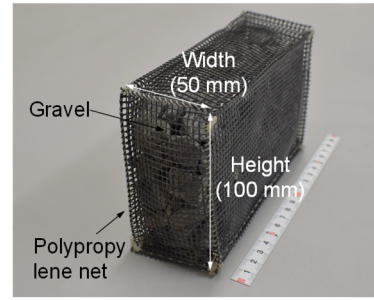


Fig. 4 Photograph of geogrid gabion model.

Table 1 Experimental cases considered.

	Initial horizontal distance, D_h	Thrust force, F [N]
Case N2	—	149
Case G3	0.3D	149–254
Case G4	1.0D	149–277
Case G6	2.0D	149–301

D: pipe diameter of 50 mm.

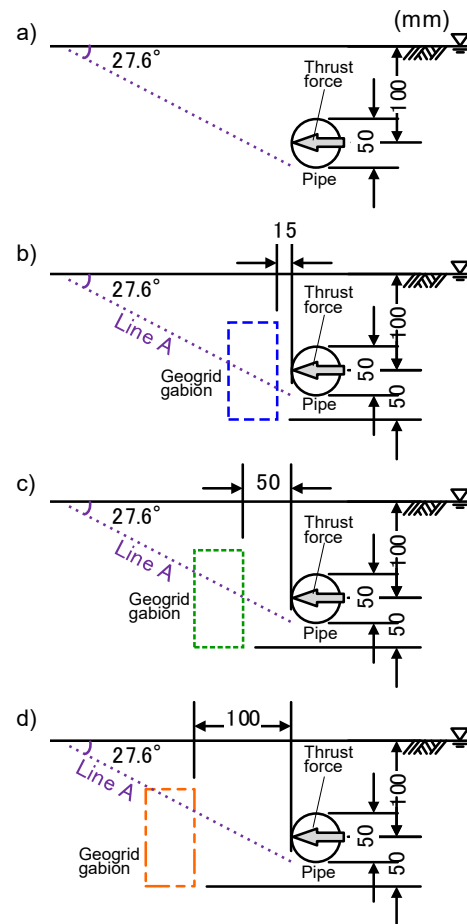


Fig. 5 Schematic layout of the pipe and the geogrid gabion; a) case N2, b) case G3, c) case G4, and d) case G6.

displacement converged. The same procedure was repeated with a stepwise increase in the value of F .

The values of σ_p , u_p , and d_p were measured under the loading of the simulated thrust force. The experiment was finished when the value of σ_p began to decrease. For case G6, the experiment was finished when the pipe displacement converged under a load F of 301 N because the pipe displacement reached the limit of the loading device.

Aluminum markers with a diameter of 7 mm were embedded in the side of the ground model beforehand, and the displacement of the markers following the deformation of the ground was observed by analyzing the images taken from the side of the testing box. The maximum shear strain γ_{max} in the ground model was calculated for each four-node rectangular element using four markers.

3. TEST RESULTS AND DISCUSSION

3.1 Pipe Displacement and Resistance

Fig. 6 shows the relationships between F and d_p just before unloading in each step. It can be seen that, in case N2, the pipe displacement with a loading of 149 N increases to nearly 30 mm. In the other cases with the geogrid gabion under 149 N loading, the pipe displacements are lower than those in case N2. Under loading of 200 N or less, the d_p value in case G3 is small compared to those in cases G4 and G6, which indicates that the pipe displacement is highly restrained when the initial distance between the pipe and the geogrid gabion is small. It should be noted that the d_p value in case G3 significantly increases under loading of 254 N.

Figure 7 shows the relationships between σ_p and d_p during loading. Assuming that the surface friction of the pipe model is small owing to the smooth surface of the pipe, most of the resistance to the thrust force is due to the passive earth pressure. In this study, the value of σ_p is used as a representative indicator of the resistance acting on the pipe model, although σ_p was measured in a small area on the side of the pipe model.

From Fig. 7, it can be seen that in case N2 without a geogrid gabion, the σ_p value reaches its peak at approximately 8 kPa and then gradually decreases. In contrast, in the cases with a geogrid gabion, the peak values of σ_p are larger than that in case N2, and the slopes of the σ_p and d_p relationships decrease as D_h increases. It should be noted that the relationship between σ_p and d_p in case G6 might have trended upward continuously if a thrust force larger than 301 N had been applied.

Figure 8 shows the relationships between the peak σ_p and d_p at the peak values of σ_p . The peak values of σ_p in cases N2, G3, G4, and G6 are 8.7 kPa, 26.9 kPa, 22.9 kPa, and 15.5 kPa, respectively.

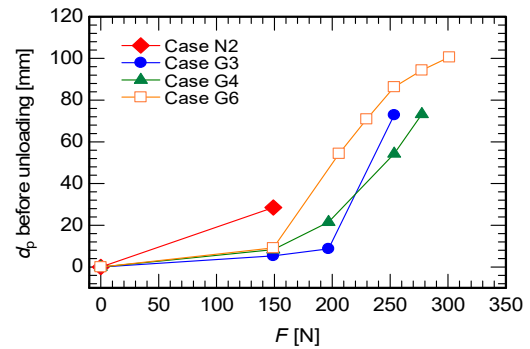


Fig. 6 Relationships between F and d_p just before unloading in each step.

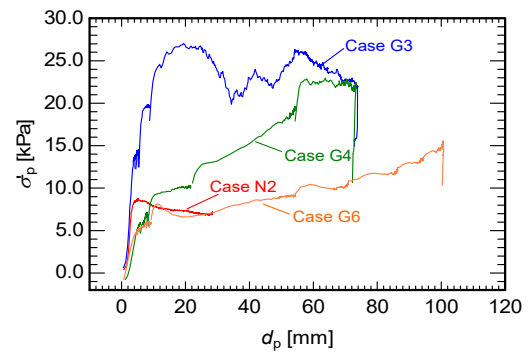


Fig. 7 Relationships between σ_p and d_p .

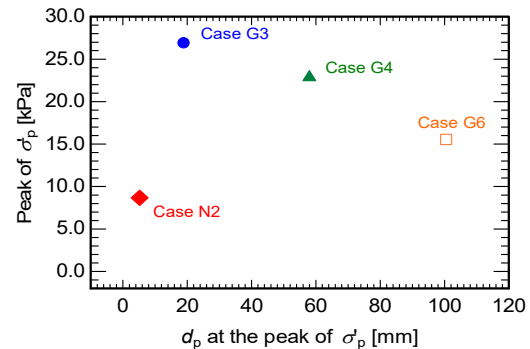


Fig. 8 Relationships between the peak values of σ_p and d_p at the peak values of σ_p .

It should be noted that the value of σ_p in case G6 might not be reached the peak as mentioned before. The peak values of σ_p in cases G3, G4, and G6 are more than approximately twice that in case N2. It is clear that the resistance acting on the pipe model is increased when the geogrid gabion is installed.

Figure 9 shows the relationship between d_p at the peak values of σ_p and D_h . The d_p values at the peak values of σ_p are approximately the same as the value of D_h . This indicates that the resistance acting on the pipe is highest when the pipe model approaches the geogrid gabion.

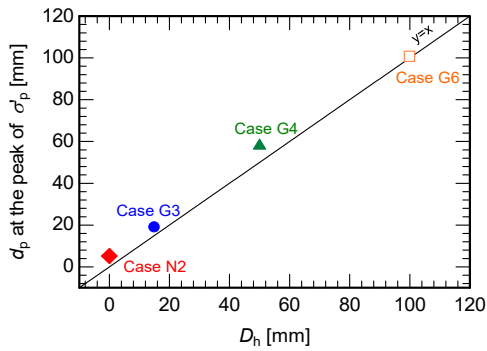


Fig. 9 Relationships between d_p at the peak values of σ'_p and D_h .

3.2 Ground Deformation

Fig. 10 shows the distributions of γ_{max} in the ground when the pipe displacement is approximately 20 mm. The thrust force was applied in the left direction in all cases.

In case N2, the band of high shear strain is distributed from the left side of the pipe model to the ground surface, which indicates that the boundary of the passive area in the ground (Fig. 10a). The band of high shear strain on the right side of the pipe model is the active area of the ground.

In case G3, the geogrid gabion moves by approximately 19 mm horizontally, and the shear strain increases from the bottom of the geogrid gabion to the ground surface (Fig. 10b). This indicates that the geogrid gabion resists the thrust force received from the pipe, and the passive area in the ground is larger than that in case N2. This geogrid gabion is located across the boundary of the passive area of the pipe model (Fig. 5b), and the thrust force is probably transmitted to the geogrid gabion smoothly.

In case G3, the effective value of the lateral earth stress acting on the pipe reaches its peak value when the pipe displacement is 19 mm (Fig. 8), which was observed under a loading F of 254 N (Fig. 6). When the pipe displacement is 19 mm, a band of a high shear strain of approximately 30% formed in the passive area in contact with the geogrid gabion (Fig. 10b), and the stress state in the band is assumed to be in the residual state. The thrust force of 254 N seems to exceed the resistance force, and therefore, the pipe displacement significantly increases from 9 to 73 mm upon a loading F of 254 N.

In contrast, a high strain band appears in between the pipe and geogrid gabion in case G6 (Fig. 10d). Most of the geogrid gabion is located outside the passive area in contact with the pipe model; subsequently, the thrust force is assumed to be hardly transmitted to the geogrid gabion at this time. Hence, the resistance to the thrust force is

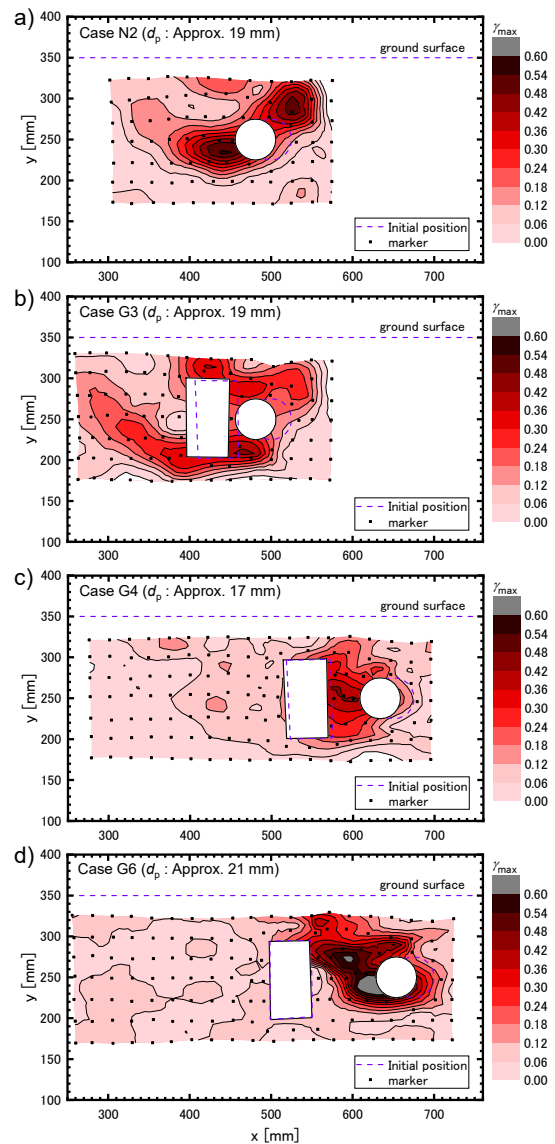


Fig. 10 Distribution of maximum shear strain at a d_p of approximately 20 mm; a) case N2, b) case G3, c) case G4, and d) case G6.

mainly due to the passive earth pressure acting on the pipe model. This is also supported by the fact that the relationship between σ'_p and d_p in case G6 is similar to that in case N2 at d_p below approximately 20 mm (Fig. 7).

In case G4, although a high shear strain band appears between the pipe and geogrid gabion, the shear strain slightly increases in the passive area in contact with the geogrid gabion (Fig. 10c). Therefore, the thrust force is assumed to be slightly transmitted to the geogrid gabion through the passive area of the pipe. The σ'_p value in case G4 is larger than that in case N2 and G6 when the pipe displacement is approximately 20 mm, as shown in Fig. 7, probably because the passive earth pressure acting on the geogrid gabion also acts as a resistance.

3.3 Resistance by Geogrid Gabion

Figure 11 shows a schematic of the resistance force in the thrust-protection using a geogrid gabion based on the experimental results. The resistance force to thrust force is modeled as the sum of the passive earth pressure acting on the pipe and the resistance increment provided by the geogrid gabion.

When the value of D_h is as small as $0.3D$, the thrust force from a pipe is transferred quickly to a geogrid gabion. Therefore, the resistance force increases even when the pipe displacement is small. In contrast, when D_h is greater than $1.0D$, the resistance is due to the passive earth pressure mainly acting on the pipe when the pipe displacement is small. As the pipe approaches the geogrid gabion, the thrust force is transmitted to the geogrid gabion; subsequently, the resistance due to the passive earth pressure acting on the geogrid gabion increases gradually. The resistance force acting on the pipe is highest when the pipe displacement approaches the value of D_h .

The increase in resistance is assumed to depend on the size of the pressure-receiving area of the geogrid gabion. Under the experimental conditions in this paper, the height of the geogrid gabion is 100 mm, which is twice the diameter of the buried pipe model. The total force of the passive earth pressure acting on the pressure-receiving area can be calculated to be two times larger when the pressure-receiving area is two times larger. The geogrid gabion is subjected to frictional resistance generated by its upper and lower surfaces, which is also expected to increase further the resistance force. Therefore, the maximum values of the resistance with the geogrid gabions are estimated to be more than approximately twice that without the geogrid gabions, regardless of the value of D_h .

While the above discussion is based on the results of experiments using a scaled model, the actual buried pipes are larger in diameter and deeper in burial depth than that of the model. It should be noted that the effects of the burial depth and the scale factor should be verified for applying this idea of the resistance force in the thrust-protection using a geogrid gabion to actual buried pipes.

4. CONCLUSIONS

The use of a geogrid gabion as a thrust-protection method for buried pipes was tested on a model with different initial distances between the geogrid gabion and the pipe. The conclusions are summarized as follows:

- 1) The peak resistance force of the pipe with the geogrid gabion was more than approximately twice that of the pipe without the geogrid gabion,

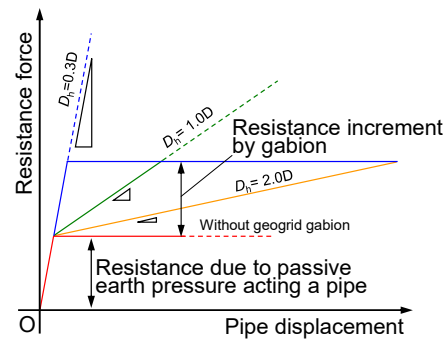


Fig. 11 Schematics of the resistance force by using geogrid gabion.

regardless of the initial horizontal distance between the geogrid and the pipe, under the experimental conditions in this paper.

- 2) When the initial horizontal distance was as small as $0.3D$, the resistance force rapidly increased even when the pipe displacement was small. In cases where the initial horizontal distance was more than $1.0D$, the resistance force acting on the pipe gradually increased as the pipe displacement increased.
- 3) The values of the pipe displacement at the peak values of the effective lateral stress acting on the pipe model were approximately the same as the value of the initial horizontal distance. In other words, the resistance force acting on the pipe was highest when the pipe approached the geogrid gabion.
- 4) As the pipe approached the geogrid gabion, the thrust force was transmitted to the geogrid gabion; subsequently, the resistance due to the passive earth pressure acting on the geogrid gabion was gradually provided to the pipe.
- 5) The resistance force was modeled as the sum of the passive earth pressure acting on the pipe and the resistance increment provided by the geogrid gabion.

5. ACKNOWLEDGMENTS

The authors would like to thank Mr. Nichiri Kusunose and Mr. Kotaro Nagamori (former undergraduate students at Kagawa University), for their help with conducting the model experiments. This study was supported by JSPS KAKENHI Grant Number 19K15090.

6. REFERENCES

- [1] Mohri Y., Yasunaka M. and Tani S., Damage to Buried Pipeline Due to Liquefaction Induced Performance at the Ground by the Hokkaido Nansei-Oki Earthquake in 1993, Proceedings of First International Conference on

- Earthquake Geotechnical Engineering, IS-Tokyo, 1995, pp. 31–36.
- [2] Mohri Y., Ono S. and Suzuki K., Seismic Damage to Large-Diameter Pipelines, *The Foundation Engineering & Equipment*, Vol.48, No.1, pp. 40–43, 2020. (in Japanese)
- [3] Kawabata T., Sawada Y., Uchida K., Hirai T. and Saito K., Model Tests on Thrust Protecting Method for Buried Bend with Geogrid, *Geosynthetics Engineering Journal*, Japan Chapter of International Geosynthetics Society, Vol. 19, 2004, pp. 59–64. (in Japanese)
- [4] Kawabata T., Sawada Y., Ogushi K., Totsugi A., Hironaka J., Mohri Y. and Uchida K., Large-Scale Experiments on Pipe Bend with Lightweight Thrust Restraint Using Geogrid, *Geosynthetics Engineering Journal*, Japan Chapter of International Geosynthetics Society, Vol. 21, 2006, pp. 105–110. (in Japanese)
- [5] Kawabata T., Sawada Y., Mohri Y. and Ling I., Dynamic Behavior of Buried Bend with Thrust Restraint in Liquefying Ground, *Journal of Japanese Society of Civil Engineering*, Vol.67, No. 3, 2011, pp. 399–406. (in Japanese)
- [6] Araki H. and Hirakawa D., Model Tests on Thrust Protecting Method for Buried Pipe by Using Geogrid Gabion, *Journal of Japanese Society of Civil Engineering*, Vol. 74, No. 1, 2018, pp. 106–117. (in Japanese)
- [7] Araki H. and Hirakawa D., Effects of Thrust Protecting Method for Buried Pipe Using Geogrid Gabion of Different Sizes, *International Journal of GEOMATE*, Vol. 16, No. 158, 2019, pp. 62–68.
- [8] Itani Y., Fujita N., Sawada Y., Ariyoshi M., Mohri Y. and Kawabata T., Model Experiment on the Horizontal Resistance Force of Buried Pipe in Liquefied Ground, *Irrigation, Drainage and Rural Engineering Journal*, Vol. 295, 2015, pp. 77–83. (in Japanese)
- [9] Japanese industrial standards, JIS A 1210:2020, Test Method for Soil Compaction Using a Rammer.
- [10] Japanese geotechnical society standards, JGS 0524-2009, Method for Consolidated-Drained Triaxial Compression Test on Soils.

Copyright © Int. J. of GEOMATE. All rights reserved, including the making of copies unless permission is obtained from the copyright proprietors.
